

## Supramolecular Chemistry

# A Terrylene Bisimide based Universal Host for Aromatic Guests to Derive Contact Surface-Dependent Dispersion Energies

Jessica Rühe, Megha Rajeevan, Kazutaka Shoyama, Rotti Srinivasamurthy Swathi, and Frank Würthner\*

Dedicated to Professor Julius Rebek, Jr. on the occasion of his 80th birthday

**Abstract:**  $\pi$ - $\pi$  interactions are among the most important intermolecular interactions in supramolecular systems. Here we determine experimentally a universal parameter for their strength that is simply based on the size of the interacting contact surfaces. Toward this goal we designed a new cyclophane based on terrylene bisimide (TBI)  $\pi$ -walls connected by *para*-xylylene spacer units. With its extended  $\pi$ -surface this cyclophane proved to be an excellent and universal host for the complexation of  $\pi$ -conjugated guests, including small and large polycyclic aromatic hydrocarbons (PAHs) as well as dye molecules. The observed binding constants range up to  $10^8 \text{ M}^{-1}$  and show a linear dependence on the 2D area size of the guest molecules. This correlation can be used for the prediction of binding constants and for the design of new host-guest systems based on the herewith derived universal Gibbs interaction energy parameter of  $0.31 \text{ kJ/mol}\text{\AA}^2$  in chloroform.

Host-guest complexes offer the opportunity to study intermolecular interactions between molecules and to elucidate important processes found in nature such as substrate binding by receptors or catalysis by enzymes.<sup>[1]</sup> Therefore, the design of host structures for the molecular recognition of interesting guest molecules<sup>[2]</sup> continues to attract researchers in their endeavor to utilize such complexes as functional supramolecular entities. From the very beginning the class of cyclophanes has received special attention<sup>[3]</sup> and in particular the ‘Blue Box’ (Figure 1) introduced by Stoddart and co-workers in 1988<sup>[4]</sup> has demonstrated a wide scope of applications by taking advantage of the combination of substrate binding and redox processes for the development of molecular machines.<sup>[5]</sup> Most noteworthy design concepts of the Blue Box are the *para*-xylylene spacers providing an

ideal distance for the accommodation of aromatic guests and the positively charged 4,4'-bipyridinium units whose electron-poor nature is supportive for the binding of electron-rich aromatic guests and accessible for reductive redox switching.<sup>[6]</sup> Considering such a breakthrough example for a functional cyclophane and its narrow scope for small-sized guests, it is rather surprising that it took 25 years until the first expanded derivative, the so-called ExBox<sup>4+</sup>, was presented in 2013 with its ability to encapsulate a larger variety of aromatic guests.<sup>[7]</sup> In the following years, many other extended box- and cage-shaped hosts have been reported based on the linkage of benzene and pyridinium units.<sup>[8]</sup> However, the expansion of the aromatic building blocks into the second dimension, thereby enlarging the  $\pi$ -surface of the host, has been less explored.<sup>[9]</sup> Different from these examples based on positively charged hosts our group is interested since some time in neutral cyclophanes based on functionally-rich rylene bisimide dyes<sup>[10]</sup> and their complexes with polycyclic aromatic hydrocarbons (PAHs).<sup>[11]</sup> Whilst our initial cyclophane designs based on perylene bisimide (PBI) units did not afford the desired open cavities for guest encapsulation due to the strong intermolecular interactions between the larger  $\pi$ -planes of these dyes,<sup>[12]</sup> in 2015 we finally accomplished the synthesis of the first PBI cyclophane acting as a host for various PAHs.<sup>[13]</sup> Still, however, due to the restricted length of the PBI moiety the cavity of this and other meanwhile reported PBI cyclophanes<sup>[14]</sup> remains rather small, enabling only binding of a limited number of guests such as perylene with high affinity as required for photophysical studies on such host-guest complexes in dilute solution. To overcome this deficiency, here we introduce a new cyclophane comprising of larger terrylene bisimide (TBI) moieties.<sup>[15]</sup> The expansion compared to previously reported hosts is illustrated in

[\*] J. Rühe, Dr. K. Shoyama, Prof. Dr. F. Würthner  
Institut für Organische Chemie  
Universität Würzburg  
Am Hubland, 97074 Würzburg, Germany  
E-mail: wuerthner@uni-wuerzburg.de

M. Rajeevan, Dr. R. S. Swathi  
School of Chemistry  
Indian Institute of Science Education and Research Thiruvananthapuram (IISER TVM)  
Vithura, Thiruvananthapuram 695551, India

Dr. K. Shoyama, Prof. Dr. F. Würthner  
Center for Nanosystems Chemistry (CNC)  
Universität Würzburg  
Theodor-Boveri-Weg, 97074 Würzburg, Germany

© 2024 The Authors. Angewandte Chemie International Edition published by Wiley-VCH GmbH. This is an open access article under the terms of the Creative Commons Attribution License, which permits use, distribution and reproduction in any medium, provided the original work is properly cited.

Figure 1. For this cyclophane we demonstrate strong binding of an unprecedented variety of PAHs and dyes, and reveal the influence of substituents on binding affinities. Based on this data set we provide general insights into dispersion forces and derive a parameter for the estimation of binding strengths for future receptor designs for  $\pi$ -conjugated molecules simply based on the size of the interacting van der Waals surfaces.<sup>[16]</sup>

The synthetic route to TBI cyclophane **TBI-C** commences by the build-up of the unsubstituted TBI **1** based on a recently improved synthetic protocol from our laboratory.<sup>[17]</sup> Afterwards solubilizing aryloxy substituents are attached by bromination and nucleophilic substitution following the procedure reported by Müllen and co-workers to receive **TBI-ref** (Scheme S1).<sup>[18]</sup> Diisopropylphenyl imide substituents are then removed by saponification, leading to terrylene bisanhydride **2** (Scheme 1).<sup>[19]</sup> By reaction with Boc-protected *para*-xylenediamine, deprotection and subsequent cyclization with **2** the cyclophane **TBI-C** could be obtained in quite good yields of 52% considering the competitive formation of open-chained oligomers and polymers as well as larger sized macrocycles. The strategy of using such protected linkers for the cyclization was previously developed in our group for the synthesis of heterocyclophanes,<sup>[14c]</sup> but showed also to increase the yields for the synthesis of homo-cyclophanes compared to the formerly applied one-step method.<sup>[13]</sup> For details on the experimental procedures and characterization of all new compounds, see the Supporting Information.

Single crystal X-ray analysis of **TBI-C** crystals grown from di-*n*-butyl ether solution by slow vapor diffusion of methanol give us insight into the structural details (Fig-

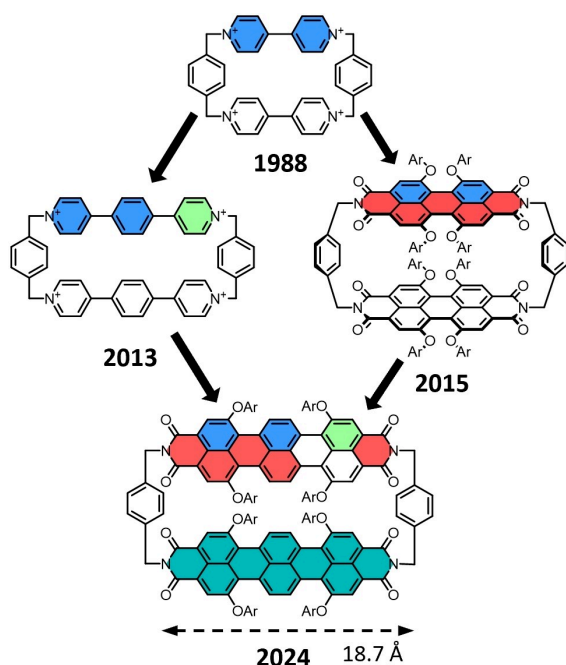
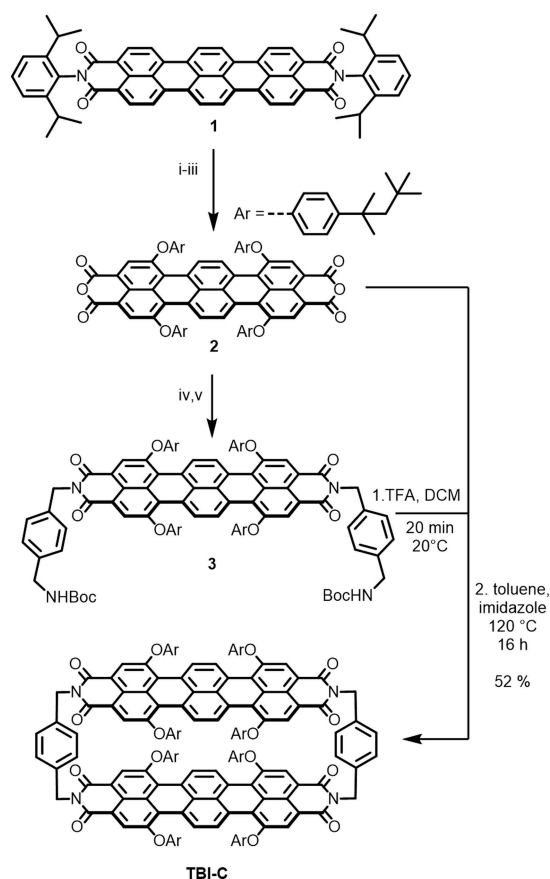


**Figure 1.** Overview over previously published cyclophane hosts and their relationship to the herein newly presented terrylene bisimide cyclophane.



**Scheme 1.** a) Synthetic route to **TBI-C** with i)  $\text{Br}_2$ , chlorobenzene/ $\text{H}_2\text{O}$ ,  $50^\circ\text{C}$ , 17 h, 81%; ii) *tert*-octylphenol,  $\text{K}_2\text{CO}_3$ , NMP,  $80^\circ\text{C}$ , 5 h, 88%; iii) KOH, KF, *tert*-butanol,  $80^\circ\text{C}$ , 4 h, 43%; iv) *N*-Boc-*para*-xylenediamine, toluene/imidazole,  $120^\circ\text{C}$ , 16 h, 75%; v) TFA,  $\text{CH}_2\text{Cl}_2$ , room temperature, 30 min, quantitative. NMP: *N*-methyl-2-pyrrolidone, TFA: Trifluoroacetic acid, Boc: *tert*-butoxycarbonyl.

ure 2).<sup>[20]</sup> Accordingly, this cyclophane exhibits an almost perfect box-shaped structure with both TBI moieties being positioned parallel to each other at an interchromophoric distance of ca.  $6.7\text{ \AA}$  that is perfectly suited for the encapsulation of planar guest molecules.<sup>[7]</sup> Indeed, in addition to several disordered solvent molecules outside of the cavity one di-*n*-butyl ether molecule is embedded in the cavity. For the unsubstituted model compound **TBI-C(H)** (without OAr substituents, see Figure S42) and di-*n*-butyl ether an attractive interaction energy of  $-43.1\text{ kJ/mol}$  was calculated (Figure S43). Compared to other known cyclophanes, the dimensions of the **TBI-C** cavity are very spacious with a length of about  $18.7\text{ \AA}$  and a width of  $6.4\text{ \AA}$ , corresponding to the TBI's  $\pi$ -surface area of  $120\text{ \AA}^2$ . Pleasingly, the four *tert*-octyl-functionalized phenoxy substituents are protruding to the exterior and exert little distortion of the TBI  $\pi$ -planes.

The optical properties of cyclophane **TBI-C** were studied by UV/Vis absorption and fluorescence spectroscopy in comparison to the reference dye **TBI-ref** (Figure S7). The decrease of the  $A_{0-0}/A_{0-1}$  ratio in the main UV/Vis absorption band at  $550\text{--}750\text{ nm}$  from 1.97 for **TBI-ref** to 1.17 for **TBI-C**

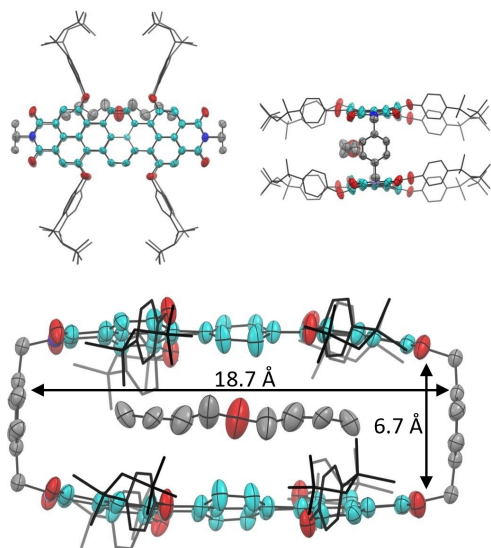


**Figure 2.** Molecular structure of cyclophane **TBI-C** obtained by single crystal X-ray analysis from the top, side, and front view. Ellipsoids are drawn at 50% probability. Substituents are heavily disordered and only the major part is displayed in stick model. Hydrogen atoms and solvent molecules outside of the cavity are omitted for clarity.

in chloroform indicates a substantial H-type coupling between the TBI chromophores.<sup>[21]</sup> Emission spectroscopy reveals a weak fluorescence in the near infrared (NIR) spectral region in chloroform ( $\Phi_f \sim 1.2\%$ ) for **TBI-C** that is significantly increased in toluene ( $\Phi_f \sim 40\%$ ). All spectroscopic data are summarized in Table S1.

The crystal structure shown in Figure 2 commends TBI cyclophane as an ideal host for the encapsulation of planar aromatic guests. Thus, titration experiments with a variety of  $\pi$ -conjugated guest molecules were performed. A favorable feature of the blue-colored TBI chromophore for such studies is provided by its main absorption band being positioned at the long-wavelength edge of the visible range where most PAHs and dyes are not absorbing. Accordingly, guest uptake by **TBI-C** in titration experiments can be monitored easily by the changes in the absorbance of this band by UV/Vis absorption spectroscopy. Figure 3 shows the host–guest titration experiment of **TBI-C** host in chloroform using the red-colored diindenoperylene as a guest. Upon stepwise addition of the guest a decrease and bathochromic shift of the TBI absorption band is observed. The titration data could be fitted with the 1:1 binding model to give the high binding constant of  $K_a = 4.73 \times 10^5 \text{ M}^{-1}$ .

For the diindenoperylene $\subset$ **TBI-C** complex single crystals could be grown by vapor diffusion of *n*-hexane into a chloroform solution of **TBI-C** and excess diindenoperylene.<sup>[20]</sup> The co-crystals were analyzed by single crystal X-ray diffraction to afford the structure depicted in Figure 4. Accordingly, diindenoperylene occupies the whole **TBI-C** cavity and is indeed rotationally displaced ( $32^\circ$ ) as it is slightly too long to fit parallelly in the cavity. The interacting  $\pi$ -surfaces of the host and the guest are nevertheless substantial, thereby explaining the observed high binding constant.

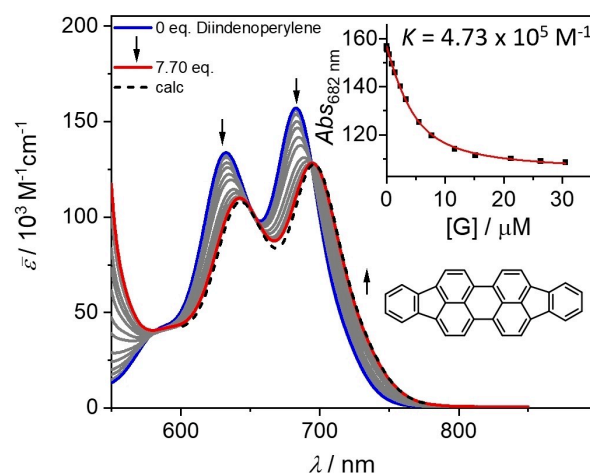


**Figure 3.** UV/Vis absorption spectra of **TBI-C** in  $\text{CHCl}_3$  at  $20^\circ\text{C}$  ( $c = 4.0 \times 10^{-6} \text{ M}$ ) upon the addition of diindenoperylene. The dashed line shows the calculated spectrum for the 1:1 complex calculated from global-fit analysis. Inset: The resulting plot of the absorption at  $\lambda = 682 \text{ nm}$  with nonlinear curve fit (1:1 binding model, red curve).

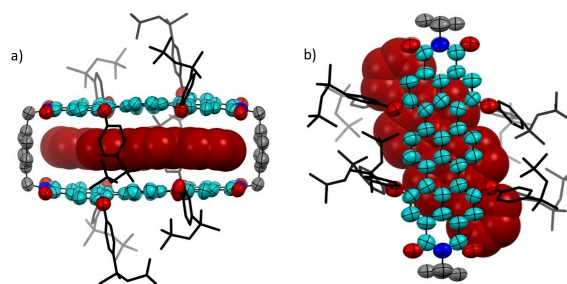


**Figure 4.** Molecular structure of the complex diindenoperylene $\subset$ **TBI-C** obtained by single crystal X-ray analysis from the front (a) and top view (b). Ellipsoids are drawn at 50% probability. Substituents are heavily disordered and only the major part is displayed in stick model. Hydrogen atoms and solvent molecules outside the cavity were omitted for clarity. Diindenoperylene is displayed in the space-fill model in red.

To our delight, a plethora of other planar  $\pi$ -conjugated guest molecules could be encapsulated as well within the cavity provided by **TBI-C**, including unsubstituted PBIs and perylene monoimides (PMIs), dipolar merocyanine (MC) dyes, terthiophene as well as unsubstituted and halogenated PAHs. All binding studies are displayed in the Supporting Information (Figures S8 to S39). To compare the binding strength of the cyclophane for the variety of guests in chloroform at 293 K, Figure 5a shows the usual approach where the logarithm of the binding constant (or the related Gibbs free binding energy) is related to the number of  $\pi$ -electrons of the guest molecules. Such correlations have been shown for a variety of aromatic hosts such as Stoddart's pyridinium-based cyclophanes,<sup>[7]</sup> Yam's metallosupramolecular tweezers<sup>[22]</sup> or our PBI cyclophanes,<sup>[13]</sup> for guest molecules with small enough size for being accommodated in the respective cavities. Figure 5a shows that this correlation is also valid for the new TBI cyclophane with embedded pristine aromatic molecules (data in black).

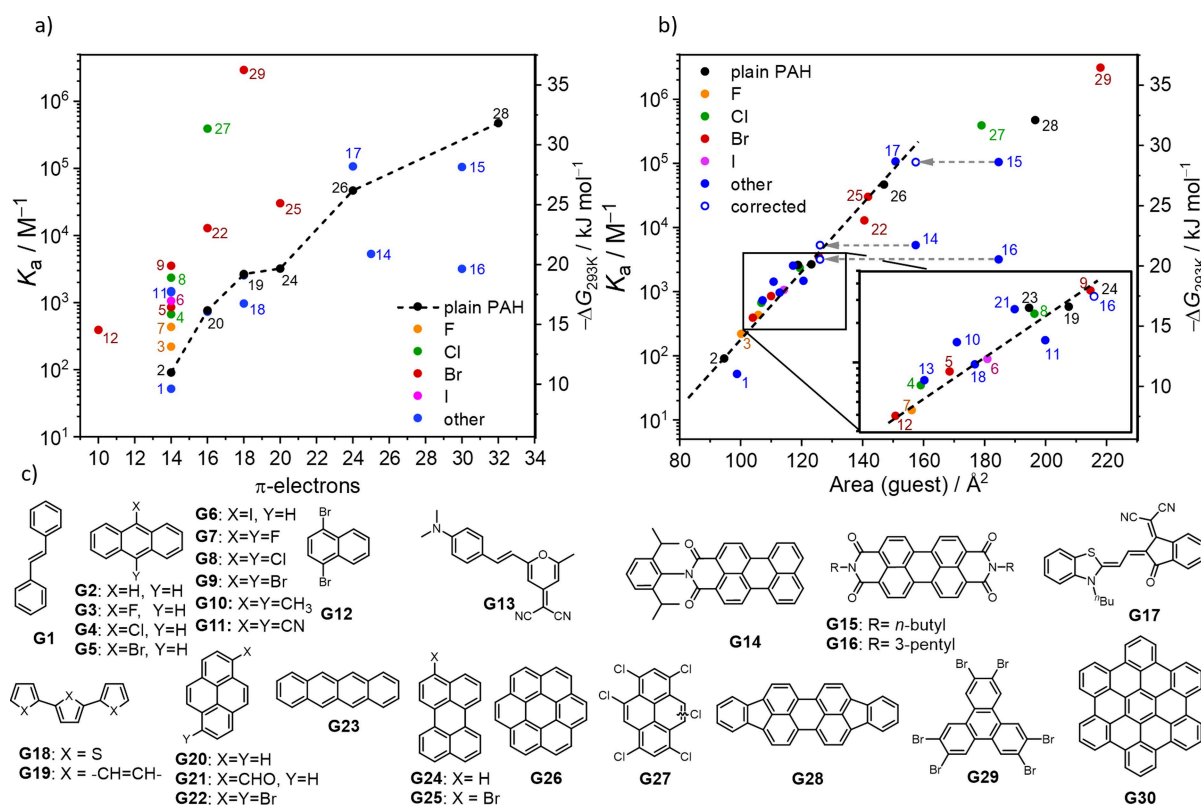


**Figure 5.** Plot of binding constants  $K_a$  for the complexation of  $\pi$ -conjugated guest molecules **GX** by **TBI-C** versus the number of their  $\pi$ -electrons (a) and the guest's surface area (b) according to UV/Vis absorption spectroscopy titration experiments in chloroform at 293 K. The arrows and hollow circles in b) represent the corrected data points after consideration of the limited area of guests **G14–G16** that can be encapsulated. In c) the chemical structures of all guests **GX** are depicted with their numbers.

However, many of the data points for substituted PAHs and several dye molecules are far off this correlation. Because the binding for these molecules is mostly enhanced, the substituents obviously provide additional binding strength that is not included in the simple  $\pi$ -electron count approach. An improved method for the determination of the surface area of the respective guests is accordingly based on the van der Waals surface extracted from molecular modelling (for further details, see Supporting Information). Based on this observation, we plotted all experimental binding data in relation to the surface area of the respective guests (Figure 5b).

Remarkably, this facile approximation of size-dependent binding of guests also works for the halogenated guests and for guests deviating from the simple PAH structure such as **G3–G9**, **G13**, **G17**, and **G18**. Accordingly, our novel expanded molecular box of **TBI-C** provides unprecedented experimental insights regarding the intermolecular interaction forces provided by planar two-dimensional  $\pi$ -surfaces, here TBI, towards various  $\pi$ -conjugated guests. For instance, due to sufficient space provided by **TBI-C** for the various anthracenes we can easily elucidate how the replacement of hydrogen by halogen atoms as well as increasing their numbers affords an increase of binding strength (Figure S37). Remarkably, the increase of binding affinity is more pronounced when going from anthracene ( $K_a = 9.08 \times 10^1$  M $^{-1}$ ) to dibromoanthracene ( $K_a = 3.54 \times 10^3$  M $^{-1}$ )

than upon annulation of another ring as in tetracene as a guest ( $K_a = 2.61 \times 10^3$  M $^{-1}$ ). We like to emphasize that no halogen bonding is involved in this case but that the increase in binding strength is originating merely from an increase of dispersion interactions due to the highly polarizable halogen substituents.<sup>[23]</sup> The assumption that dispersion forces between the aromatic  $\pi$ -system of TBI and highly polarizable halogen atoms account for the observed effect is substantiated by the binding strength for at 9-position substituted and at 9- and 10-disubstituted anthracenes that increases in the series  $H < F < CH_3 < CN < Cl < Br < I$ . Clearly this finding corroborates the common observation that halogenated solvents are best suited to solubilize aromatic compounds ('*similia similibus solvuntur*') and also invigorates our appreciation for the binding constants observed for the complexes of **TBI-C** for the herein investigated compounds in the solvent chloroform. The increased binding for nitrile and methyl substituted anthracenes can also be explained by larger dispersion interactions. The complexes of halogenated anthracenes with **TBI-C(H)** have also been elucidated by density functional theory (DFT) calculations and the trend of interaction energies shows good correspondence to the experimental binding energies (Figure S45). This also implies that the solubilizing side chains of the host are not significantly affecting the binding behavior as they were removed for the calculations.



Taking a closer look at the perylene (bis)imides that were studied as guests, it is observed that they deviate significantly from the linear correlation presented in Figure 5b. This, however, can be easily understood: For the perylene mono- and bisimides (**G14–G16**) the encapsulation of the entire PBI/PMI core is unrealistic as the steric demands of the imide substituent(s) enforces their protrusion out of the cavity, thereby limiting the amount of  $\pi$ -contact surface with the host molecule. If only the embedded surface area of the guest molecules according to semiempirical calculations (Figure S41) is considered, the observed binding constants are located on the linear curve (as marked with the arrows in Figure 5b). For very large guests such as hexabromotriphenylene (**G29**), hexachloropyrene (**G27**) and diindenoperylene (**G28**, compare Figure 4), it is also obvious that not the whole surface of the guest can be covered by the TBI  $\pi$ -surface and therefore the binding constants are lower than expected from the linear correlation. A specific size limitation for guest molecules as observed for capsules (Rebek's 55 % rule)<sup>[24]</sup> is not apparent, presumably due to the open edges of our cyclophane. Among our series of studied guests, the highest precisely determined binding constant of  $2.93 (\pm 0.38) \times 10^6 \text{ M}^{-1}$  has been observed for hexabromotriphenylene (**G29**). The complexation of hexabenzocoronene (**G30**, **HBC**) was also studied and UV/Vis titrations and NMR studies (Figure S40) in chloroform showed complexation. The binding constant was, however, not determinable by UV/Vis titration studies due to **HBC**'s poor solubility in this solvent. In toluene, where the high fluorescence quantum yield of **TBI-C** and the better solubility of **HBC** make fluorescence titrations possible a binding constant of  $1 \times 10^8 \text{ M}^{-1}$  was determined. As in toluene the binding constants of other guests are decreased compared to chloroform (e.g. 3-bromoperylene:  $1.04 \times 10^3 \text{ M}^{-1}$  in toluene vs.  $3.04 \times 10^4 \text{ M}^{-1}$  in chloroform, Figure S41) a binding constant of  $\geq 10^8 \text{ M}^{-1}$  would be expected for **HBC** in chloroform. This is a remarkably high value for a dispersion interaction based complex in a good solvent as most complexes of neutral guests bound with a micromolar affinity so far took advantage of solvophobic effects.<sup>[25]</sup>

Finally, our large data set allowed us to calculate the Gibbs binding energy per interacting van der Waals surface ( $A$ ) by a surface size-related parameter  $\sigma = -\Delta G^\circ/A$  from the linear fit shown in Figure 5b. This leads to a value of  $\sigma = 0.31 \text{ kJ/mol}\text{\AA}^2$  for interacting  $\pi$ -conjugated van der Waals surfaces in chloroform.<sup>[26]</sup> This value should be considered as a lower limit because it has been derived for chloroform which is a very good solvent for aromatic  $\pi$ -surfaces. Accordingly, an increase in other solvents and in particular for the gas phase is expected.<sup>[27]</sup> Still, compared to the interaction energy reported for highly dipolar merocyanines with  $\sigma$  up to  $1.3 \text{ kJ/mol}\text{\AA}^2$  in dioxane<sup>[28]</sup> this is a lower value, thereby emphasizing the important role of electrostatic dipole–dipole interactions between merocyanines at close  $\pi$ – $\pi$ -contact distances. DFT-calculations for the interaction energies of plain PAHs with **TBI-C(H)** corroborate the linear correlation with the surface area of the guest (Figure S44a). Further, natural energy decomposition analysis

(NEDA)<sup>[29]</sup> performed for these complexes reveals the most important contributions to the binding interaction (Figure S44b) that are, as expected from the cavity design, exchange-correlation (in which dispersion is included) and polarization as the most stabilizing components.<sup>[30]</sup>

In conclusion, a new expanded molecular box with a very large  $\pi$ -surface area has been introduced. Titration studies supported by X-ray crystal structures show its suitability for the encapsulation of planar aromatic guests ranging from small up to very large size and reaching binding affinities up to  $10^8 \text{ M}^{-1}$ . From a linear relationship between the Gibbs binding energies and the van der Waals contact surfaces between this host and a large variety of guests we were able to derive the surface size-related interaction energy parameter  $\sigma = 0.31 \text{ kJ/mol}\text{\AA}^2$  in chloroform that might be quite useful for future receptor designs. Further, considering such a large substrate scope for TBI complexes and the exciting photofunctional features encoded in TBIs<sup>[31]</sup> the cyclophane holds promise for a variety of projects to be addressed in the future.

## Supporting Information

The data underlying this study is available in the Supporting Information and in Zenodo at <https://doi.org/10.5281/zenodo.10213572>.

## Acknowledgements

We thank the Cusanuswerk for a PhD scholarship for J.R. We acknowledge DESY (Hamburg, Germany), a member of the Helmholtz Association HGF, for providing experimental facilities at PETRA III (proposal No I-20211168 and I-20220338). We thank Dr. Eva Crosas and Dr. Guillaume Pompidor for assistance in using P11. M.R. and R.S.S. acknowledge use of the Padmanabha cluster at the Centre for High-performance Computing at IISER TVM. R.S.S. acknowledges the Science and Engineering Research Board (SERB), Government of India for financial support, through the SERB Core Research Grant (CRG/2022/006873). M.R. thanks IISER TVM for her fellowship. Open Access funding enabled and organized by Projekt DEAL.

## Conflict of Interest

The authors declare no conflict of interest.

## Data Availability Statement

The data that support the findings of this study are openly available in Zenodo at <https://doi.org/10.5281/zenodo.10213572>.

**Keywords:** Cyclophanes • Terrylen Bisimide • Host-Guest systems • Dispersion force • Dye complexation

- [1] a) S. Kubik, *Supramolecular Chemistry*, Walter de Gruyter GmbH, Berlin/Boston **2021**, p.468; b) J. W. Steed, J. L. Atwood, *Supramolecular Chemistry*, 3rd ed., John Wiley & Sons Ltd, Hoboken **2022**, pp. 381–383.
- [2] a) J.-M. Lehn, *Angew. Chem.* **1988**, *100*, 91–116, *Angew. Chem. Int. Ed. Engl.* **1988**, *27*, 89–112; b) J.-M. Lehn, *Angew. Chem.* **1990**, *102*, 1347–1362; *Angew. Chem. Int. Ed. Engl.* **1990**, *29*, 1304–1319.
- [3] F. Diederich, *Angew. Chem.* **1988**, *100*, 372–396; *Angew. Chem. Int. Ed. Engl.* **1988**, *27*, 362–386.
- [4] B. Odell, M. V. Reddington, A. M. Z. Slawin, N. Spencer, J. F. Stoddart, D. J. Williams, *Angew. Chem.* **1988**, *100*, 1605–1608; *Angew. Chem. Int. Ed. Engl.* **1988**, *27*, 1547–1550.
- [5] V. Balzani, A. Credi, F. M. Raymo, J. F. Stoddart, *Angew. Chem.* **2000**, *112*, 3484–3530; *Angew. Chem. Int. Ed.* **2000**, *39*, 3348–3391.
- [6] R. A. Bissell, E. Cordova, A. E. Kaifer, J. F. Stoddart, *Nature* **1994**, *369*, 133–137.
- [7] J. C. Barnes, M. Juríček, N. L. Strutt, M. Frascioni, S. Sampath, M. A. Giesener, P. L. McGrier, C. J. Bruns, C. L. Stern, A. A. Sarjeant, J. F. Stoddart, *J. Am. Chem. Soc.* **2013**, *135*, 183–192.
- [8] a) E. J. Dale, N. A. Vermeulen, M. Juríček, J. C. Barnes, R. M. Young, M. R. Wasielewski, J. F. Stoddart, *Acc. Chem. Res.* **2016**, *49*, 262–273; b) I. Roy, A. H. G. David, P. J. Das, D. J. Pe, J. F. Stoddart, *Chem. Soc. Rev.* **2022**, *51*, 5557–5605.
- [9] a) X. Gong, J. Zhou, K. J. Hartlieb, C. Miller, P. Li, O. K. Farha, J. T. Hupp, R. M. Young, M. R. Wasielewski, J. F. Stoddart, *J. Am. Chem. Soc.* **2018**, *140*, 6540–6544; b) X. Gong, R. M. Young, K. J. Hartlieb, C. Miller, Y. Wu, H. Xiao, P. Li, N. Hafezi, J. Zhou, L. Ma, T. Cheng, W. A. Goddard, O. K. Farha, J. T. Hupp, M. R. Wasielewski, J. F. Stoddart, *J. Am. Chem. Soc.* **2017**, *139*, 4107–4116.
- [10] a) R. K. Dubey, F. Würthner, *Nat. Chem.* **2023**, *15*, 884; b) Y. Avlasevich, C. Li, K. Müllen, *J. Mater. Chem.* **2010**, *20*, 3814–3826.
- [11] P. Spenst, F. Würthner, *J. Photochem. Photobiol. C* **2017**, *31*, 114–138.
- [12] F. Schlosser, M. Moos, C. Lambert, F. Würthner, *Adv. Mater.* **2013**, *25*, 410–414.
- [13] P. Spenst, F. Würthner, *Angew. Chem.* **2015**, *127*, 10303–10306; *Angew. Chem. Int. Ed.* **2015**, *54*, 10165–10168.
- [14] a) M. Weh, J. Rühle, B. Herbert, A.-M. Krause, F. Würthner, *Angew. Chem.* **2021**, *133*, 15451–15455; *Angew. Chem. Int. Ed.* **2021**, *60*, 15323–15327; b) S. E. Penty, M. A. Zwiijnenburg, G. R. F. Orten, P. Stachelek, R. Pal, Y. Xie, S. L. Griffin, T. A. Barendt, *J. Am. Chem. Soc.* **2022**, *144*, 12290–12298; c) G. Ouyang, J. Rühle, Y. Zhang, M.-J. Lin, M. Liu, F. Würthner, *Angew. Chem.* **2022**, *134*, e202206706; *Angew. Chem. Int. Ed.* **2022**, *61*, e202206706.
- [15] L. Chen, C. Li, K. Müllen, *J. Mater. Chem. C* **2014**, *2*, 1938–1956.
- [16] S. Grimme, J. Antony, T. Schwabe, Christian Mück-Lichtenfeld, *Org. Biomol. Chem.* **2007**, *5*, 741–758.
- [17] K. Shoyama, M. Mahl, S. Seifert, F. Würthner, *J. Org. Chem.* **2018**, *83*, 5339–5346.
- [18] F. Nolde, J. Qu, C. Kohl, N. G. Pschirer, E. Reuther, K. Müllen, *Chem. Eur. J.* **2005**, *11*, 3959–3967.
- [19] S. Wieghold, J. Li, P. Simon, M. Krause, Y. Avlasevich, C. Li, J. A. Garrido, U. Heiz, P. Samori, K. Müllen, F. Esch, J. V. Barth, C.-A. Palma, *Nat. Commun.* **2016**, *7*, 10700.
- [20] Deposition Numbers 2310187 (for **TBI-C**) and 2310188 (for diindenoperylene-**TBI-C**) contain the supplementary crystallographic data for this paper. These data are provided free of charge by the joint Cambridge Crystallographic Data Centre and Fachinformationszentrum Karlsruhe Access Structures service.
- [21] a) F. C. Spano, *Acc. Chem. Res.* **2010**, *43*, 429–439; b) J. Rühle, D. Bialas, P. Spenst, A.-M. Krause, F. Würthner, *Org. Mater.* **2020**, *02*, 149–158.
- [22] Y. Tanaka, K. M.-C. Wong, V. W.-W. Yam, *Chem. Eur. J.* **2013**, *19*, 390–399.
- [23] U. Mayerhöffer, F. Würthner, *Angew. Chem.* **2012**, *124*, 5713–5717; *Angew. Chem. Int. Ed.* **2012**, *51*, 5615–5619.
- [24] S. Mecozzi, J. Rebek Jr., *Chem. Eur. J.* **1998**, *4*, 1016–1022.
- [25] S. Sarkar, P. Ballester, M. Spektor, E. A. Kataev, *Angew. Chem.* **2022**, *135*, e202214705; *Angew. Chem. Int. Ed.* **2023**, *62*, e202214705.
- [26] In our calculation we have assumed that the  $\pi$ -surfaces of both TBIs are in close contact to the guest and accordingly contribute to the measured binding constant. Because this might not be the case, i.e. due to not perfect distance, the calculated value for  $\sigma$  is accordingly a lower limit.
- [27] F. Würthner, *J. Org. Chem.* **2022**, *87*(3), 1602–1615.
- [28] F. Würthner, *Acc. Chem. Res.* **2016**, *49*, 868–876.
- [29] E. D. Glendening, *J. Am. Chem. Soc.* **1996**, *118*(10), 2473–2482.
- [30] H.-J. Schneider, *Acc. Chem. Res.* **2015**, *48*, 1815–1822.
- [31] R. M. Young, M. R. Wasielewski, *Acc. Chem. Res.* **2020**, *53*, 1957–1968.

Manuscript received: December 1, 2023

Accepted manuscript online: February 28, 2024

Version of record online: March 18, 2024